A STUDY OF AMBIENT VIBRATIONS FOR PIEZOELECTRIC ENERGY CONVERSION

Elizabeth K. Reilly, Lindsay M. Miller, Romy Fain, and Paul Wright
Mechanical Engineering, University of California Berkeley, Berkeley, CA

Abstract: This paper will focus on vibration to electrical energy conversion via piezoelectric materials. In order to get a more accurate picture of the amount of available energy present in ambient environmental sources a comprehensive study of vibrations found in industrial, residential, and various other setting was done. The sources have been organized into five categories with respect to frequency: noise, broadband, impact, low frequency, resonant spike. This information was then used in modeling the expected power output of an energy harvester.

Keywords: ambient vibrations, piezoelectric, energy harvesting

INTRODUCTION

Energy harvesting has gained attention over the last several years as energy requirements of low-power electronics have decreased and the need for a renewable wireless power supply has increased. The goal is for energy harvesting to ultimately replace finite sources of energy, such as batteries, extending the lifetime of the electronic device and eliminating the need for maintenance. Sources of ambient energy include, for example, solar, thermal, vibration, and wind energy. Vibrations are an attractive source of harvestable energy because they are ubiquitous in the built environment, are found in a large variety of locations, and are relatively easy to convert to usable electrical energy.

The harvestable energy that is available from vibrations in the environment is not usually in the form of a single sinusoidal signal. Most previous research focuses on an idealized single sinusoidal input, which is valuable for obtaining insight into the behavior of the system but is not sufficient for understanding how a real vibration energy harvesting device would behave subjected to an ambient vibration source. The present work will identify and characterize ambient vibrations available for conversion. We will then present a power output estimate based on measured ambient vibrations of an HVAC duct using piezoelectric conversion.

EXPERIMENTAL

A vibration study was completed using Microstrain G-link accelerometers. The vibration sources have been organized into five categories with respect to frequency: noise, broadband, impact, low frequency, and resonant spike [Table 1]. Usable sources were determined using the following criteria: frequency spike at or above 0.01*g*, resultant of 2 or 3 axes spikes of the same frequency at or above 0.01*g*, broadband optimizable, or very low frequencies at or above 0.1*g*. Notable sources include the refrigerator, computer/server, poster printer, HVAC system, electric tea pot, air compressor, walking/running, and driving.

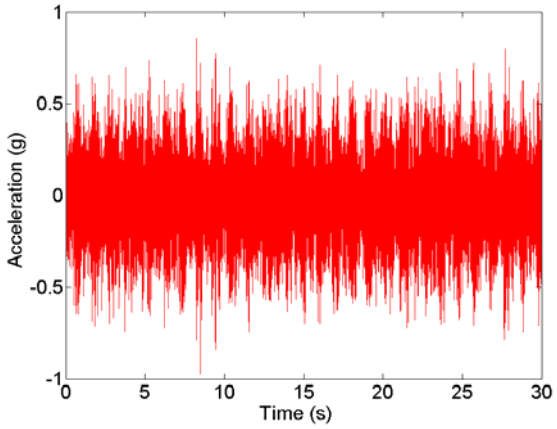

Figure 1: Acceleration profile of HVAC duct

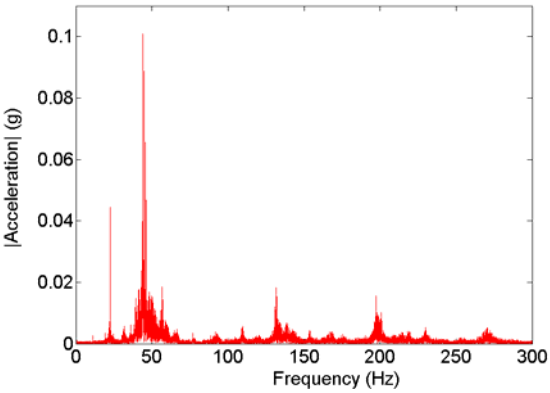

Figure 2: Fast Fourier Transform (FFT) of the HVAC duct vibrations

Table 1: A survey of ambient vibrations

	Frequency (Hz)	Acceleration (*g*'s)	Resultant of # axes		Characterization
Statasys 3D printer	28.0	0.044	1		s
	28.3	0.060	2		s
	44.7	0.017	3		s
W500 Lenovo laptop	119.0	0.199	3		s
	85.2	0.205	3		s
	119.0	0.141	1		s
	85.2	0.158	1		s
Milwaukee Cordless Drill	0.2	1.080	2		i
	15.2	0.363	2		s
External HD	119.3	0.014	3		s
	119.3	0.012	1		s
Washing Machine	85.0	0.314	3		s
	85.0	0.287	1		s
Rockwell Sander	59.3	0.121	1		s
	92.5	0.138	1		s
Monarch Lathe Splatter Guard	15.5	0.069	2		s
	24.5	0.052	2		s
Monarch Lathe Chassis	284.0	0.144	3		bb
Delta Drill Press	41.3	0.407	1		s/bb
	184.8	0.172	2		s/bb
Delta Vertical Bandsaw	122.5	0.140	1		s/bb
HVAC Roof	184.5	0.252	2		bb
	184.5	0.236	1		bb
HVAC Vent	21.8	0.469	1		bb
	29.0	0.344	1		bb
	127.3	0.214	1		bb
Driving 2002 Toyota Camry	0.2	0.210	2		i
	42.8	0.022	1		bb
	24.0	0.073	1		bb
Scraper Bike	0.2	0.091	2		i
	15.0	0.062	1		s/bb
Running	1.5	2.045	2		s/lf
	5.1	0.762	1		s/lf
Walking	1.0	0.430	3		s/bb/lf
	3.7	0.305	1		s/bb/lf
Portable Home Air-compressor	43.7	2.103	1		s
Refrigerator	58.7	0.018	3		s
Electric Tea Pot	241.0	0.019	2		bb
Poster Printer	92.5	0.200	3		s
Server/computer	35.3	0.016	1		s

Characterization key is as follows: s = resonant spike, bb = broadband optimizable, i = impact (<1 Hz), lf = low frequency (<10 Hz). Noise and very low frequencies have been excluded. Resultant accelerations from more than one axis were only included if the contributing axes were maximum frequencies.

Figures 1 and 2 illustrate the vibration data from an HVAC duct in detail. The data was collected in the same way as the data in Table 1. Figure 1 presents the acceleration versus time and Figure 2 shows the acceleration versus frequency. It can be seen that the dominant acceleration peaks are at approximately 22 and 45 Hz.

THEORETICAL MODEL

A significant amount of research has gone into developing an accurate model of piezoelectric conversion subjected to a single sinusoidal vibration input. Williams and Yeats [2] presented the first model of transduction based on electromagnetic transductions. Subsequent models [3-6] have refined their basic principles and produced a more accurate result. Halvorsen [7] presented an analytical model of energy harvester response to broadband vibrations.

In this paper we use the model developed by Roundy and Wright [8] to predict power output from a piezoelectric energy harvester subjected to the input vibrations from the HVAC duct shown in Figures 1 and 2. We use the four most dominant frequency peaks as inputs to the model to obtain an estimated voltage and power output.

The equivalent circuit model for a piezoelectric vibration energy harvesting system is shown in Figure 3. In this model, the harvester is an equivalent mass, L_m, spring, C_k, and damper, R_b, with the electromechanical coupling modeled as a transformer. The load is idealized as a resistor. The full derivation will not be provided here but is explained, in detail, in [8].

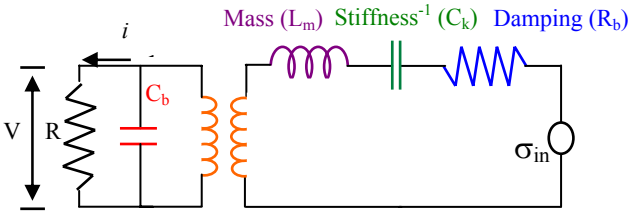

Figure 3: Circuit representation of a piezoelectric generator with a resistive load.

From the circuit diagram in Figure 3, Kirchhoff's voltage and current laws can be used to obtain two Equations, (1) and (3), respectively. Substitution results in both equations in terms of strain and voltage as seen in Equations (2) and (4), and details of this procedure can be found elsewhere [8].

$$\sigma_{in} = \sigma_m + \sigma_b + \sigma_k + nV \tag{1}$$

$$\ddot{S} = \frac{-c_p}{k_1 k_2 m} S - \frac{b_m}{m}\dot{S} + \frac{c_p d_{31}}{k_1 k_2 m t_p} V + \frac{\ddot{y}}{k_2} \tag{2}$$

$$i = i_C + i_R \tag{3}$$

$$\dot{V} = \frac{t_p c_p d_{31}}{\varepsilon}\dot{S} - \frac{1}{RC_p} V \tag{4}$$

Where σ is stress, which is analogous to voltage. n is the transformer turns ratio, V is voltage, S is strain, which is analogous to charge, c_p is stiffness of piezoelectric layer, k_1 and k_2 are given in Equations (6) and (7). Furthermore, m is proof mass, b_m is mechanical damping coefficient, t_p is thickness of piezoelectric layer, d_{31} is the piezoelectric coefficient, y is input vibration displacement, i is current, C_p is the capacitance of the piezoelectric layer, R is the optimum load resistance, and ε is dielectric constant.

The analytical expression for power transferred to a resistive load can be developed by using Equations (2) and (4) to substitute voltage for strain in order to obtain an equation for voltage, which is given in Equation (5). The average power dissipated by the resistive load is simply $P = |V|^2/2R$. From Roundy and Wright [8] the output voltage is:

$$V = \frac{j\omega \frac{c_p d_{31} t_p A_{input}}{\varepsilon k_2}}{\left[\frac{\omega_n^2}{RC_p} - \left(\frac{1}{RC_p} + 2\xi\omega_n\right)\omega^2\right] + j\omega\left[\omega_n^2\left(1+k_{31}^2\right) + \frac{2\xi\omega_n}{RC_p} - \omega^2\right]} \tag{5}$$

Where A_{in} is the input acceleration magnitude, ω_n is the resonant frequency of the cantilever, ζ is the total damping ratio, and k_2, k_2 and k_{31} are as follows:

$$k_1 = \frac{t_p}{2I}(2L_b + L_m - L_e) \tag{6}$$

$$k_2 = \frac{L_b^2}{t_p}\frac{(\frac{2}{3}L_b + \frac{1}{2}L_m)}{(2L_b + L_m - L_e)} \tag{7}$$

$$k_{31} = \sqrt{\frac{d_{31}^2 c_p}{\varepsilon_{33}}} \tag{8}$$

L_b, L_m, and L_e represent length of beam, mass, and electrode, respectively, and I is the moment of inertia. The variables used in the model are listed in Table 2.

Table 2: Model parameters

Parameter	Value	Parameter	Value
L_{beam}	3.5 mm	E_{piezo}	194 GPa
L_{mass}	2.5 mm	E_{sio2}	80 GPa
$L_{electrode}$	L_b+L_m	E_{si}	170 GPa
W	500 μm	ε	4.9e-9 F/m
t_{piezo}	850 nm	d_{31}	50e-12 m/V
t_{si}	525 μm	C_p	40 nF
t_{pt}, t_{pd}	160 nm	R	500kΩ
t_{sifilm}	250 nm	ω_n	31 Hz
t_{sio2}	1.4 μm	ζ	0.08
E_{pt}	170 GPa		

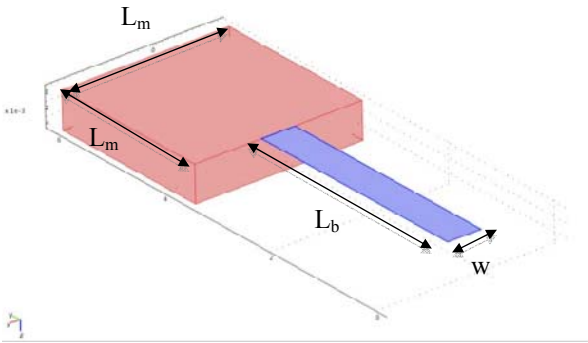

Figure 4: Geometry of piezoelectric cantilever with proof mass[1].

Figure 4 shows the geometry of the piezoelectric energy harvester used in the model. The theoretical voltage output signal expected from the beam is illustrated in Figure 5, based on the cantilever shown in Figure 4 with material parameters from Table 2 and input vibrations from an HVAC duct as given in Figures 1 and 2. The vibrations used as inputs to the model reflect the environmental frequencies and accelerations of what is found from the HVAC duct.

The average voltage output predicted for the cantilever mounted on the duct is 300 mV_{rms}. This more accurately reflects the voltage output researchers should expect from an ambient vibration source than a single sinusoidal input. The expected power produced by a single piezoelectric cantilever over a simple resistor is 0.17 μW, with a power density of approximately 10 $\mu W/cm^3$.

CONCLUSION

This paper identified specific sources of ambient vibrations and characterized their frequency spectrums and acceleration magnitudes. The vibration sources outline in this paper identified a need for a more accurate power estimation based upon a vibration input with multiple acceleration frequencies. An example power output from a MEMS fabricated piezoelectric cantilever with a proof mass excited by vibrations on an industrial HVAC duct was calculated to be approximately 10 $\mu W/cm^3$. Future work will include experimental testing of the MEMS piezoelectric scavenging devices to validate the modeling results.

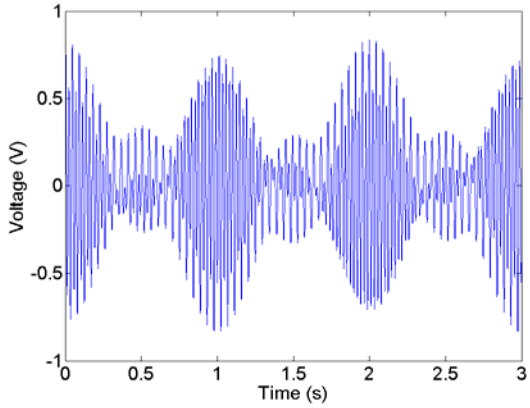

Figure 6: Theoretical voltage output from harvester

REFERENCES

[1] L. M. Miller, C. C. Ho, P. C. Shafer, P. K. Wright, J. W. Evans, R.Ramesh, (2009) Integration of a low frequency, tunable MEMS piezoelectric energy harvester and a thick film micro capacitor as a power supply system for wireless sensor nodes, *Proceedings 2009 IEEE Energy Conversion Congress and Expo*, San Jose, CA.

[2] C. B. Williams and R. B. Yates, (1996) Analysis of a micro-electric generator for microsystems, *Sensors and Actuators A*, **52** pp. 8-11.

[3] Y. C. Shu and I. C. Lien, (2006) Analysis of power output for piezoelectric energy harvesting systems, *Smart Mater. Struct.* **15** 1499–1512.

[4] A. Erturk and D. J. Inman, (2009) An experimentally validated bimorph cantilever model for piezoelectric energy harvesting from base excitations, *Smart Mater. Struct.* **18** pp. 1-18.

[5] N. G. Stephen, (2006) On energy harvesting from ambient vibration, *Journal of Sound and Vibration*, **293** pp. 409-25.

[6] N. E. duToit, B. L. Wardle, and S.-G. Kim, (2005) Design Considerations for MEMS-scale Piezoelectric Mechanical Vibration Energy Harvesters, *Integrated Ferroelectrics*, **71**pp. 121-60.

[7] E. Halvorsen, (2008) Energy Harvesters Driven by Broadband Random Vibrations, *Journal of Microelectromechanical Systems*, **17** pp. 1061-71.

[8] S. Roundy and P. K. Wright, (2004) A Piezoelectric Vibration based Generator for Wireless Electronics, *Smart Mater. Struct.* **13** pp. 1131-1142.